Effect of contact angle on the orientation, stability, and assembly of dense floating cubes

Robert Daniello, Kashan Khan, Michael Donnell, and Jonathan P. Rothstein*

Department of Mechanical and Industrial Engineering, University of Massachusetts Amherst, Amherst, Massachusetts 01003, USA

(Received 5 August 2013; published 26 February 2014)

In this paper, the effect of contact angle, density, and size on the orientation, stability, and assembly of floating cubes was investigated. All the cubes tested were more dense than water. Floatation occurred as a result of capillary stresses induced by deformation of the air-water interface. The advancing contact angle of the bare acrylic cubes was measured to be 85°. The contact angle of the cubes was increased by painting the cubes with a commercially available superhydrophobic paint to reach an advancing contact angle of 150°. Depending on their size, density, and contact angle, the cubes were observed to float in one of three primary orientations: edge up, vertex up, and face up. An experimental apparatus was built such that the sum of the gravitational force, buoyancy force, and capillary forces could be measured using a force transducer as a function of cube position as it was lowered through the air-water interface. Measurements showed that the maximum capillary forces were always experienced for the face up orientation. However, when floatation was possible in the vertex up orientation, it was found to be the most stable cube orientation because it had the lowest center of gravity. A series of theoretical predictions were performed for the cubes floating in each of the three primary orientations to calculate the net force on the cube. The theoretical predictions were found to match the experimental measurements well. A cube stability diagram of cube orientation as a function of cube contact angle and size was prepared from the predictions of theory and found to match the experimental observations quite well. The assembly of cubes floating face up and vertex up were also studied for assemblies of two, three, and many cubes. Cubes floating face up were found to assemble face-to-face and form regular square lattice patterns with no free interface between cubes. Cubes floating vertex up were found to assemble in a variety of different arrangements including edge-to-edge, vertex-to-vertex, face-to-face, and vertex-to-face with the most probably assembly being edge-to-edge. Large numbers of vertex up cubes were found to pack with a distribution of orientations and alignments.

DOI: 10.1103/PhysRevE.89.023014 PACS number(s): 47.55.nb

I. INTRODUCTION

The study of floating objects has a long history dating back to ancient Greece and the work of Archimedes. That work has principally benefitted the field of naval architecture by enabling the design of ships that can float stably under a variety of loading and weather conditions [1]. Ships and other large-scale objects float because they are less dense than water and utilize buoyancy forces [2]. Small-scale objects, however, like colloidal particles or aquatic insects, can utilize capillary forces, allowing them to float even though they are more dense than water [3–6]. For example, the legs of water striders are covered with many thousands of oriented tiny hydrophobic hairs containing nanogrooves which make them superhydrophobic with an advancing contact angle upward of $\theta_A > 150°$ [7]. Because their legs are nonwetting, the interface of the water can significantly deform under the insect's weight until the advancing contact angle is reached. The resulting capillary curvature force that far exceeds the insect's weight can be used for both floatation and locomotion [5,8,9]. By approximating the water strider's leg as a cylinder, a number of studies have investigated the effect of size, hydrophobicity, and flexibility on its performance [5,8,9]. In this paper we will try to understand the role of shape on capillary induced floating by investigating the stable orientations of and capillary forces exerted on a series of hydrophobic and superhydrophobic cubes.

Of particular interest in this study is the role that the presence and orientation of sharp edges and vertices play for cubes in capillary-induced floating. Chang *et al.* [10] showed that for objects like a vertical cylinder or a flat plate the presence of the edge at the top of the object can have a substantial effect on its ability to float. They showed that as the density of the cylinder was increased it sank deeper into the water until the contact line eventually reached the top of the cylinder, becoming pinned by the edge of the cylinder [10]. At that point, for the cylinder to sink, the interface had to be deformed such that the advancing contact angle was reached on the top, horizontal surface of the cylinder. As a result, Chang *et al.* [10] demonstrated that hydrophilic cylinders more dense than water could float due to the presence of a sharp edge. In the case of a vertical cylinder, the presence of the edge is only relevant when the cylinder is fully submerged. This is not the case for a horizontal cylinder floating on an interface. In that case, large interfacial curvature is introduced as the contact line wraps around the end of the cylinder. The presence of this curvature has little impact on the ability of the cylinders to float, but it does have a significant effect on the self-assembly of multiple cylinders floating on an interface.

Capillary interactions between multiple objects floating on an interface can lead to their self-assembly and the formation of particle rafts [11,12]. For a dense object with a large contact angle floating on the surface of a liquid, the weight of the particle can deform the fluid interface downward in such a way that the gravitation potential energy has been shown to decrease as the objects approach [13]. The result is an attractive force which scales like the inverse of particle separation and causes the floating objects to self-assemble [13]. For colloidal particles the weight of the particle becomes too small to significantly deform the fluid interface and the gravitational

*Corresponding author: rothstein@ecs.umass.edu

forces become inconsequential. Even in the absence of gravity, however, attractive interactions between particles have been observed. These attractive interactions, which are thought to be the result of electrostatic stresses caused by the particles dipolar field [14] or immersion capillary forces resulting from nonuniform wetting [13,15], can result in particle aggregation into dense clusters [15]. In addition, for these small particles suspended on an water-oil or water-air interface, Coulomb interactions can result in a repulsive force between particles that can often lead to their assembly into well-ordered hexagonal crystalline lattices [16–18].

For nonspherical particles, high interfacial curvature has been shown to cause cylindrical, ellipsoidal, and superellipsoidal particles to assemble end to end to minimize the overall interfacial curvature and energy of the system [19–22]. In addition, the presence of a sharp vertical edge, such as that produced by the edge of a square micropost, has recently been utilized to locally generate large interface curvature and template the assembly of particles on an air-water interface [19]. In this study, we investigate how floating cubes self-assemble. Of particular interest is how the presence of sharp corners and the initial floating orientation affects the resulting orientation, alignment of assemblies of multiple floating cubes, as well as the dynamics of their assembly.

II. RESULTS AND DISCUSSION

As seen by the examples in Fig. 1 and the schematic drawings in Fig. 2, cubes were observed to float in one of three primary orientations: face up, edge up, and vertex up. As we will demonstrate through both experimental measurements and theoretical predictions, the most stable capillary floating orientation is a function of the density of the cube, the size of the cube, and the contact angle made between the cube and the water.

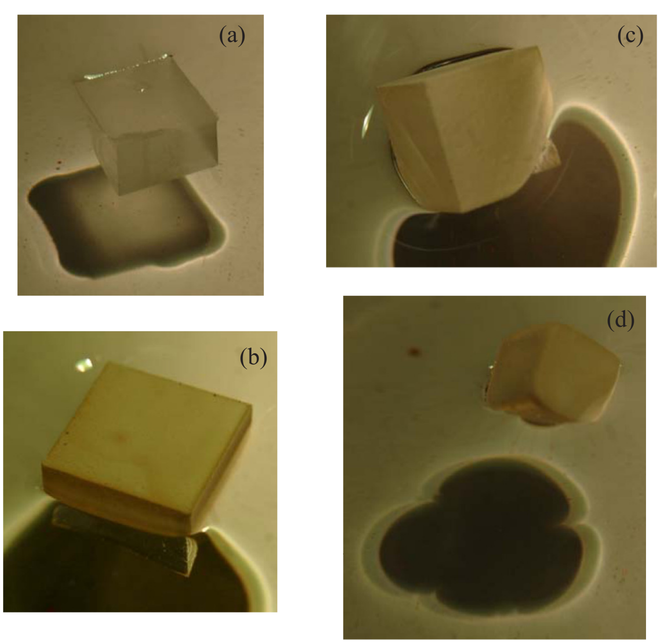

FIG. 1. (Color online) Cubes floating (a) 1 cm, $\theta = 85°$ face up, (b) 1 cm, $\theta = 150°$ face up, (c) 1 cm, $\theta = 150°$ vertex up, and (d) 6.35 mm, $\theta = 150°$ vertex up. Note that vertex up (c) and face up (b) are stable for the same 1 cm hydrophobic cube, however, vertex up is more stable.

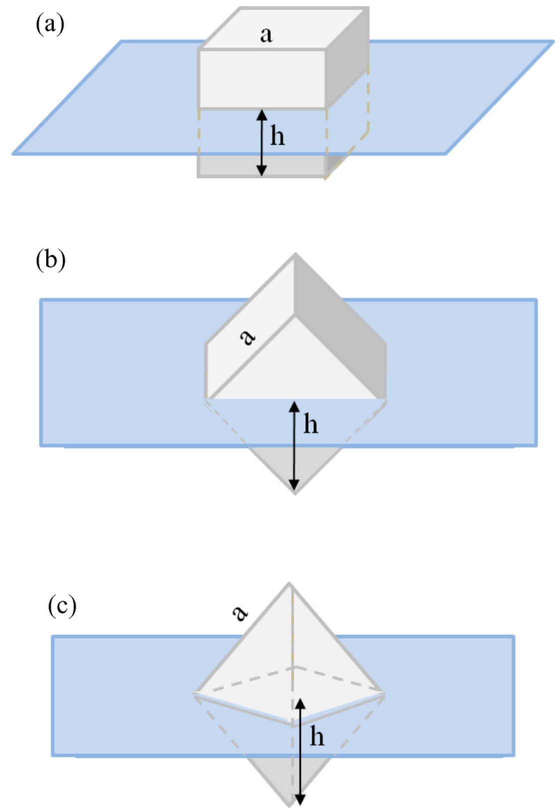

FIG. 2. (Color online) The three observed orientations of the floating cube: (a) face up, (b) edge up, and (c) vertex up.

A. Experiments

An experimental apparatus was constructed to measure the vertical forces exerted on a cube as a function of its precise depth below the free surface of a small reservoir of water. These measurements were performed to determine the equilibrium floating depth and the maximum force experienced series of acrylic cubes of different sizes, contact angles, and orientations. The force measurements were conducted with a 10g force transducer (Futek) mounted on a vertical translating stage as shown in schematically in Fig. 3. Each cube was mounted to a thin brass column which was held by a collar mounted on the force transducer. Cubes were prepared in acrylic which has a density of $\rho = 1.16$ g/cm^3 and mounted in face up, edge up, and vertex up configurations. Cubes with sides of $a = 6.35$ and 12.7 mm (McMaster Carr) were obtained commercially and $a = 1$ cm cubes were milled from blocks of acrylic. One set of cubes in each orientation was left in acrylic with an advancing contact angle $\theta_a = 85°$; while another set was prepared and coated in Fluorothane WX2100 (Cytonix, Beltsville, MD), which is a superhydrophobic coating, with an advancing contact angle of $\theta_a = 155°$. The coating thickness added less than 2% to the smallest dimensions of the cubes and does not measurably affect the density.

Cubes were individually mounted to the transducer, which was zeroed with the cube held well above the surface of the

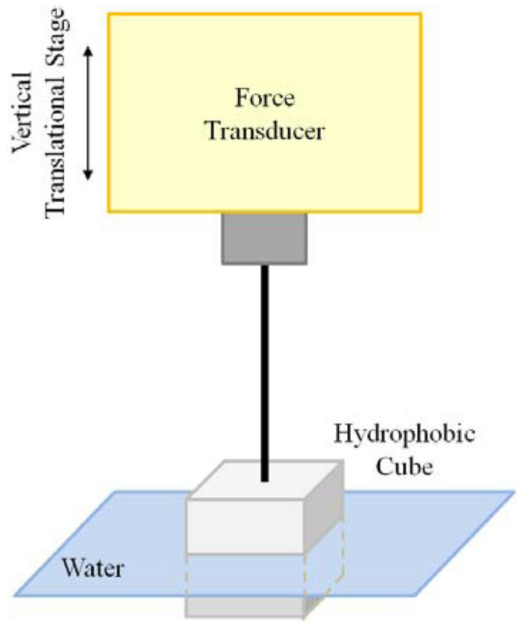

FIG. 3. (Color online) Schematic diagram of experimental setup.

water. The force transducer thus measured the sum of the capillary and the buoyancy forces on the cube. To determine the net force on the cube, the weight of the cube was subtracted from the force transducer measurements. A negative force in Figs. 4–6 thus correspond to a net downward force and a sinking cube. The cubes were brought down slowly to the point where the lowest point of the cube first contacts the water. A dial indicator with resolution of 25.4 μm was used to measure the movement of the stage; the point of first contact was set as height zero. The cube was then lowered in small increments and the force measured. Finer increments were utilized where the contact line approached edges until the cube was fully submerged. The process was repeated several times for each orientation with and without superhydrophobic coating. Additional shapes were prepared including vertical cylinders $D = 8.08$ mm with circumference equal to that of the face up cubes and a cross shape having the same perimeter as the 6.35 mm cubes with four inside edges and eight vertical outside edges. Each shape was tested with the Fluorothane WX2100 coating and in bare acrylic following the same procedure used for the cubes.

Forces on the cubes are presented in Figs. 4 and 5 for $a = 10$ mm cubes in the face, edge, and vertex up orientations and contact angles of $\theta_a = 85°$ and $\theta_a = 155°$, respectively. The results for the $\theta_a = 85°$, $a = 10$ mm cube show that only the face up orientation can float stably, as it crosses $F = 0$ mN at a depth of just over $h = 10$ mm. As a result, this cube floats with its entire body submerged below the level of the air-water interface and does so by deforming the interface that is pinned to the four edges of its vertical face. This can be seen in Fig. 1 and was observed for denser than water cylinders by Chang *et al.* [10]. That is not the case for the $\theta_a = 155°$, $a = 10$ mm cube. For this cube, as seen in Fig. 5, the buoyancy and capillary forces exerted on the cube are sufficient to allow it float in any of the three basic orientations. In all cases, the face up orientation was found to produce the largest vertical force and could therefore support the largest size or density cubes. Interestingly, for the edge up and vertex up configurations or the superhydrophobic cube, the net force on the cube crosses $F = 0$ mN at two different depths. As we will see from the simple theory presented in the next section, only the first of these two zero net force points is stable to finite perturbation. Additionally, although all three of the cube orientations were found to have a stable floating depth, our direct observations of floating cubes in Fig. 1 indicates that the vertex up orientation is the most stable. In fact, our observations are that a freely floating 10 mm superhydrophobic cube will very quickly orient itself with its vertex up independent of the orientation from which it was released. In the next section we will derive a simple theory that will explain why the vertex up orientation is the most stable for this particular cube and we will develop a stability diagram based on contact angle and cube size.

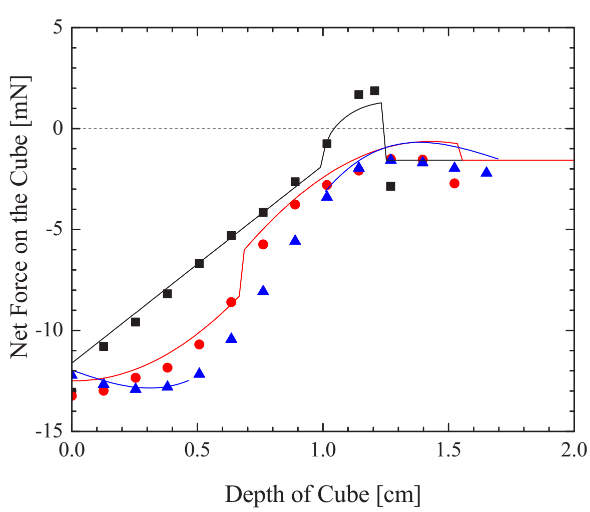

FIG. 4. (Color online) Experimental measurements of the net force as a function of vertical position for a 1 cm cube with a contact angle of $\theta = 85°$ and a density of $\rho = 1.16$ g/cm^3 oriented with (■) face up, (●) edge up, and (▲) vertex up.

B. Theory

To better understand the experimental results, a simple theory was developed to try to predict the forces exerted on a cube in different orientations and to determine the most stable orientation for floating as a function of cube density, cube size, and contact angle. For a cube to float, the capillary forces acting on the wetted perimeter of the sphere must balance the gravitational buoyancy force:

$$F_{\text{cap}} = F_g. \tag{1}$$

So that we could match the experimental measurements, the difference between the capillary forces and the gravitational forces were calculated as a function of cube position for all three observed cube orientations: face up, edge up, and vertex up.

Starting with the face up orientation, with the water interface along the vertical sides of the cube as shown in Fig. 2(a), the gravitation and capillary forces can be easily calculated by determining the length of the wetted perimeter

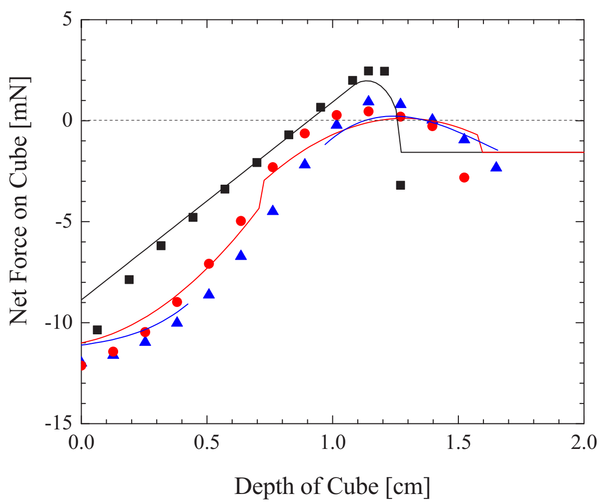

FIG. 5. (Color online) Experimental measurements of the net force as a function of vertical position for a 1 cm cube with a contact angle of $\theta = 155°$ and a density of $\rho = 1.16$ g/cm^3 oriented with (■) face up, (●) edge up, and (▲) vertex up.

and the volume of the cube submerged below the water:

$$F_g = g(\rho_w - \rho_{\text{cube}})ha^2 + g\rho_{\text{cube}}(a-h)a^2,$$
$$F_c = 4a\sigma \cos\theta. \tag{2}$$

Here σ is the interfacial tension of water, ρ_w is the density of water, ρ_{cube} is the density of cube, a is the size of the cube, h is the length of the cube submerged below the water, θ is the advancing contact angle, and g is the gravitational constant. By finding the point where the gravitational and capillary forces balance, the floating depth of the cube below the level of the water can be determined:

$$h_{\text{float}} = \frac{-(4a\sigma \cos\theta - g\rho_{\text{cube}}a^3)}{g(\rho_w - \rho_{\text{cube}})a^2 - g\rho_{\text{cube}}a^2}. \tag{3}$$

Note that Eq. (2) treats the contact line on each face of the cube independent of each other, essentially making the assumption that the presence of the vertical edge of the cube has little effect on the capillary forces. This, however, may not be true especially for small cubes where sharp corners are known to induce peaks or depressions along interfaces depending on the contact angle [23]. A full numerical simulation using surface evolver [24] would be needed to fully understand the importance of the corners, however these predictions are a useful first step that will allow us to calculate an approximate stability diagram for cubes.

As the size or density of the cube is increased, or the contact angle decreased, the equilibrium floating depth h_{float} will increase until the contact line reaches the top of the cube. At that point the contact line will becomes pinned by the edges surrounding the top face. The cube can continue to float beyond this point by deforming the air-water interface until the advancing contact angle is reached on the top face of the cube causing it to sink. Once the contact line is pinned at the edge of the top face, Eq. (2) must be modified to account for the increased deformation of the interface. Here we make another simplifying assumption on the shape of the deformed interface. In order to calculate the capillary forces, the contact angle made between the interface and the edge of the face is determined by assuming that the radius of curvature of the depressed interface is constant and set by the capillary length $L_{\text{cap}} = \sqrt{\sigma/\rho_w g}$. As a result, the contact angle made between the water and the top face of the cube can be calculated as

$$\beta = \frac{\pi}{2} - \sin^{-1}\left(\frac{L_{\text{cap}} - d}{L_{\text{cap}}}\right). \tag{4}$$

Where $d = (h - a)$ is the distance the cube has been submerged below the water level. From Eqs. (2) and (4) the force on the cube floating with the face up can be calculated as a function of position. The results are superimposed over the experimental measurements in Figs. 4 and 5 for cubes with contact angles of 85° and 155°. The results are found to match the experimental measurement reasonably well considering the number of simplifying assumptions. As seen in Figs. 4 and 5, the force is initially negative and increases roughly linearly as the cube is lowered into the water. This is a result of the decrease in the gravitational force as the cube displaces water and becomes more buoyant. At a depth of 1 cm the shape of the curve changes as the contact line is pinned by the edge of the top face of the cube. For the 85° contact angle cube, a sharp increase in the force is observed as the interface rotates from nearly horizontal on the side of the cube to nearly vertical. For the 150° contact angle cube the interface deforms and rotates through vertical as it approaches 150° causing a maximum in the force with increasing cube depth. In both cases, the face up cube can float stably as a zero net force condition can be found for both contact angles.

The predictions for the forces acting on an edge up or vertex up cube floating on water are somewhat more complicated because of the complexity of the shape. For an edge up cube, two sides are vertical and two sides are sloped at 45° angles. With the cube more than halfway submerged in the water, the forces become

$$F_g = (\rho_w - \rho_{\text{cube}})gha^2 + \tfrac{1}{2}\rho_{\text{cube}}ga^3 + (a^2 - h^2)\rho_{\text{cube}}ga,$$
$$F_c = 4h\sigma \cos\theta + 2a\sigma \cos(\theta - 45°). \tag{5}$$

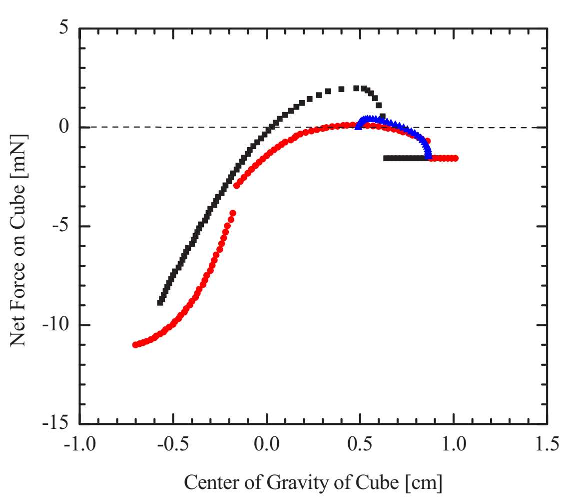

FIG. 6. (Color online) Theoretical calculations of the net force as a function of center of gravity for a 1 cm cube with a contact angle of $\theta = 155°$ oriented with (■) face up, (●) edge up, and (▲) vertex up.

Here we again treat each side of the cube independently and ignore the edge effects on the forces. For the purposes of comparison to the experimental results, the forces are also calculated when the cube is less than halfway submerged. As was the case for the face up cube, the contact line will become pinned on the horizontal edge as shown in Fig. 2(b). In our calculations we assumed the line remained pinned until the interface had been deformed such that the advancing contact angle was met on the two 45° faces. As seen in Figs. 4 and 5, our predictions show an increase in force with increasing depth and a kink in the curve when the interface becomes pinned at the horizontal edge midway up the cube. Our calculations also show that the cube will not float stably edge up with a contact angle of 85° but will with a contact angle of 155°. These predictions again match the experimental measurements very well.

Finally, calculations were performed for the cube with its vertex up. In this configuration the top of the cube becomes a trirectangular tetrahedron when all but the last 0.5 cm of the cube is submerged in the water. In this state a simple solution can be found for the gravitational and capillary forces:

$$\begin{aligned} F_g &= \tfrac{4}{3}(\rho_w - \rho_{\text{cube}})gh^3 + \left(a^3 - \tfrac{4}{3}h^3\right)\rho_{\text{cube}}g, \\ F_c &= 6\sqrt{2}h\sigma \ \cos(\theta - 45^\circ). \end{aligned} \tag{6}$$

Extending this simple theory beyond this point seemed a bit speculative because of the presence of so many edges and surfaces at different angles. Even still, this theory proved useful because as seen in Figs. 4 and 5 it was able to predict the maximum in the net force and clearly demonstrate that the cube will not float stably vertex up with a contact angle of 85° but will with a contact angle of 155°. An interesting observation for both the edge up and vertex up configuration is that unlike the face up cube, as the cube moves deeper into the water, the wetted perimeter goes down. As a result, the capillary forces go down as the cube sinks deeper into the water. This can be seen quite clearly for the case of the 155° vertex up cube. In this case, the net force has a clear maximum and crosses the zero net force line twice. Only the first of these two floating heights is stable. A cube floating at the second, lower, zero net force height will sink if it is perturbed downward from this point and move to the first zero net force height if perturbed upward.

The question then arises as to which of the three floating configurations is most stable and which configuration will the cube chose. In order to determine the stable orientation, the center of gravity was calculated for each cube orientation. The results for the 155° contact angle cube are presented in Fig. 6. The most stable orientation will be the orientation with the lowest center of gravity or the lowest gravitation potential energy when the net force on the cube is zero. Here one can observe that for a 1 cm cube with a density of 1.16 g/cm^3 and a contact angle of 155° that is the cube with the vertex up. To understand the most stable configuration for a more general case, a stability diagram was generated for cubes ranging in size from 0.5 to 1.5 cm as a function of contact angle for a fixed density of 1.16 g/cm^3. The results are shown in Fig. 7 with the experimental observations superimposed over the theoretical predictions. A similar stability diagram could be constructed with a fixed cube size and density variation as increasing density is consistent with increasing cube size.

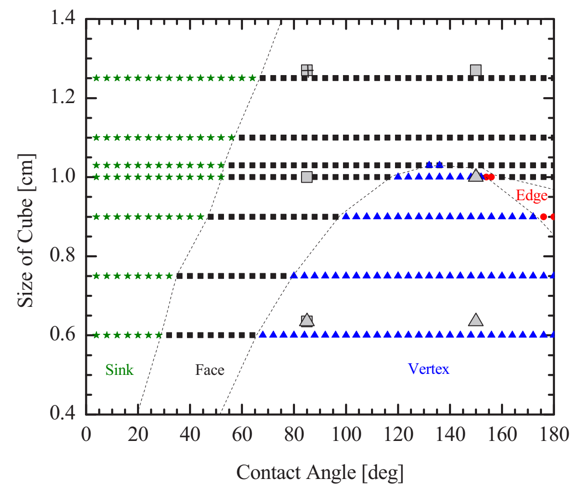

FIG. 7. (Color online) Theoretical orientation stability diagram for a cube of density $\rho = 1.16$ g/cm^3 as a function of contact angle and size of the cube. The most stable states are presented as (■) face up, (●) edge up, (▲) vertex up, or no stable state resulting in the cube sinking (★). The large filled symbols superimposed over the stability diagram at $\theta = 85°$ and 150° are the floating orientations observed in the experiments.

At low contact angles the cubes are all found to sink. The critical contact angle beyond which the cubes will float is found to increase with increasing cube size, or equivalently increasing density. In all cases, the cubes are initially found to transition from sinking to floating face up with increasing contact angle. The stability diagram shows that for cubes larger than 1.05 cm on a side, the face up orientation is the only stable floating orientation. However, below 1.05 cm, a band of vertex up orientation becomes stable at large contact angles. This band is found to broaden as the size of the cube is decreased. Interestingly, the vertex up orientation ceases to be the most stable orientation at very large contact angles for cubes close to 1 cm on a side. This is because in the vertex up configuration the angle of the cube's faces is 45° from vertical. So as the contact angle increases past 135° the vertical component of the capillary forces on the cube decreases and the vertex up cube eventually becomes unstable. At these high contact angles, a narrow band of stable edge up orientations become stable followed by the re-emergence of face up stable cubes as the contact angle gets close to 180°.

Experiments with loose cubes validate the above analysis. As seen in Fig. 7, a 12.7 mm acrylic cube with contact angle of $\theta_a = 85°$ will sink most of the time, although, with great care and a little luck, it will occasionally float face up. With $\theta_a = 155°$, the 12.7 mm acrylic cube was observed to float face up. With $\theta_a = 85°$, both the 10 and the 6.35 mm cube were observed to float face up while both of these cubes were observed to float vertex up when their contact angle was increased to $\theta_a = 155°$.

Finally, in Fig. 8 the effect of vertical edges is investigated by comparing face up cubes, face up cylinders, and face up crosses all made from acrylic with an advancing contact angle of $\theta_a = 85°$. The cube was 6.35 mm on a side. All three shapes were designed to have identical wetted perimeters and weight. Their only difference was the number of vertical edges and

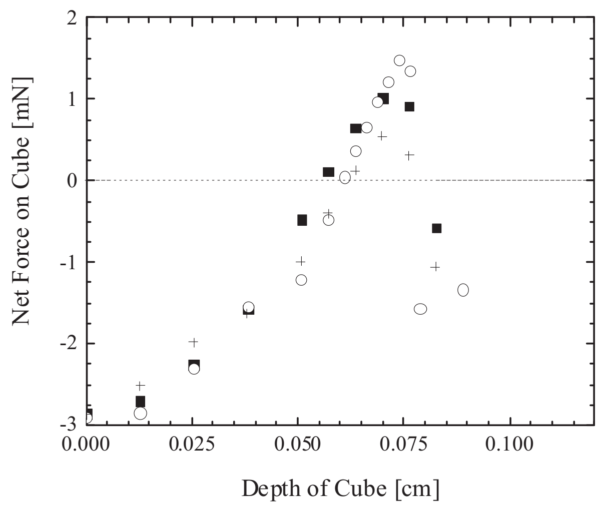

FIG. 8. Measured force as a function of height for a face up 6.35 mm cube (■), cylinder (●), and cross (+) with equal wetted perimeters $\theta = 85°$.

sharp corners present along their top faces. The presence of the sharp corners on the face of the cube and the cross was found to have a negative impact on the maximum capillary force that could be generated as the object submerged below the level of the air-water interface. The cylinder, with no vertical edges and no corners at the top face, was able to sustain the highest forces and displacements before sinking. This effect was found to develop at large depths, $h > 6.35$ mm, meaning the additional force and displacement borne by the cylinders comes as the contact line is attempting to turn the corner onto the top face of the shape. In fact, up to this point, all three shapes appear to be performing equally well. These observations indicate that the sharp corners at the top surface of the shape are destabilizing, inducing high interface curvature and providing a point of

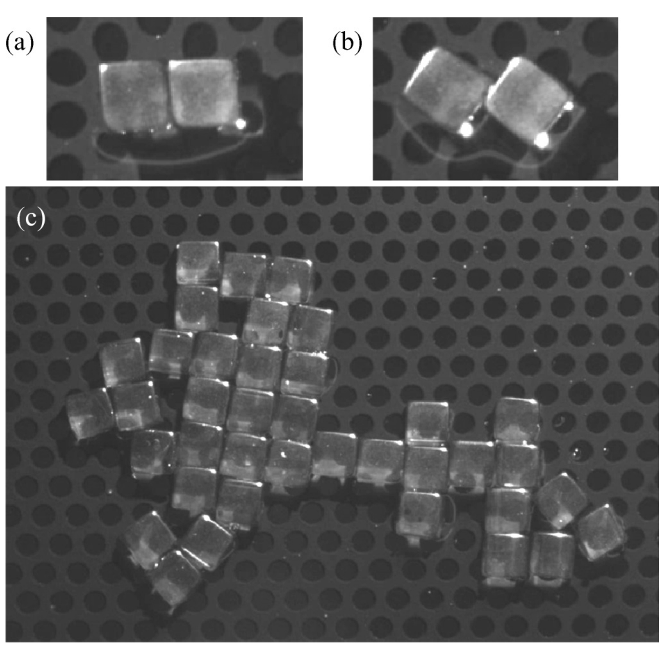

FIG. 9. Representative images for assemblies of (a) and (b) two and (c) many 0.635 mm, $\theta = 85°$ cubes floating face up.

failure from which the contact line can advance across the face causing the object to sink.

C. Assemblies of floating cubes

A series of experiments were performed to investigate the assembly of dense cubes floating at the air-water interface. In these experiments, from two to twenty 6.35 mm cubes were floated on an air-water interface and assembly process was observed. An aluminum plate with a regular array of 3.2 mm holes spaced 4.8 mm apart was used to set the initial orientation and spacing of the cubes. The cubes were arranged between 15.9 and 31.8 mm apart on center using the holes on the plate as a guide. Initial spacing was found to have little impact on the final assembly of the cubes. When studying three cubes, they

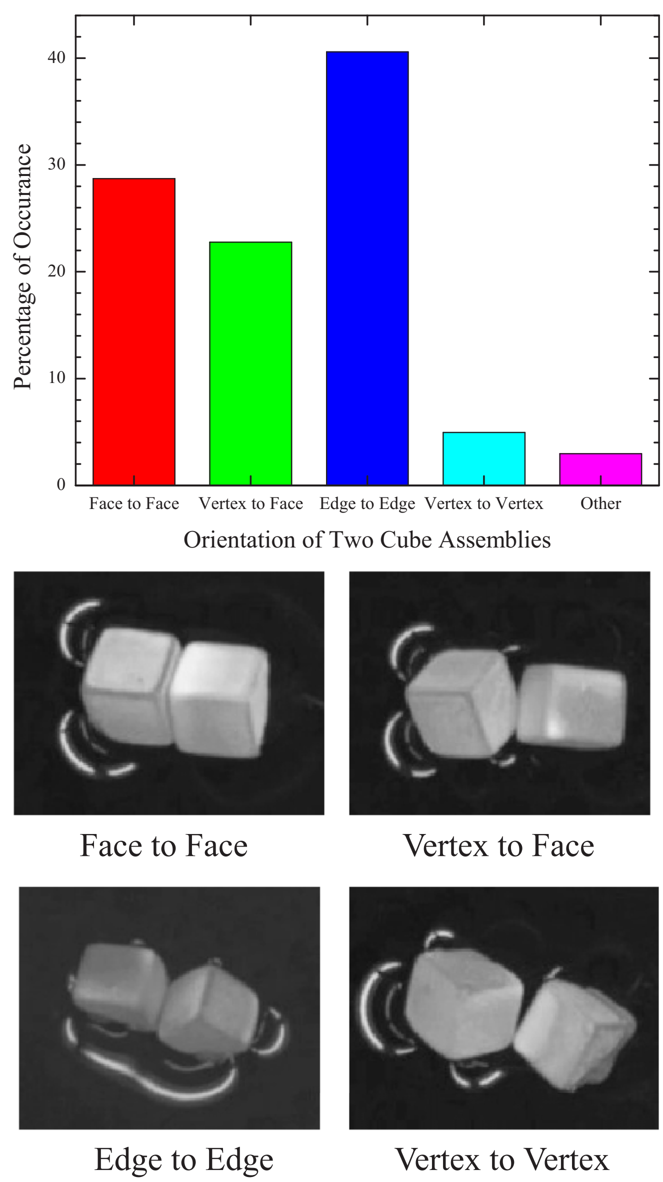

FIG. 10. (Color online) Observation frequency of two cube assemblies for the 6.35 mm, $\theta = 150°$ cubes floating vertex up. Representative images are presented for each of the four major assemblies: face-to-face, vertex-to-face, edge-to-edge, and vertex-to-vertex.

were initially arranged on the plate as an equilateral triangle, while four or more cubes were arranged as a square lattice. To insure an initial vertex up orientation for the superhydrophobic cubes, a corner of each cube was initially placed within one of the holes on the perforated plate. The plate, which can be seen in Fig. 7, was then slowly lowered into the water so that the cubes could be floated and gently released with minimal disturbance to the air-water interface.

Assemblies of cubes with an advancing contact angle of $\theta_a = 85°$, which prefer to float face up, were studied first. Independent of their initial orientation or spacing, when two face up cubes were released, they were found to rotate such that they became aligned along the diagonal of their faces as they approached each other. This is physically intuitive as the largest interfacial curvature is found near the vertical edges of the face up cubes. This also agrees with the theory developed by He *et al*. [22] who showed that the attractive force between two capillary floating object scales like $\sqrt{a/L_{\text{cap}}}$ with a proportionality coefficient that depends on the mean radius of curvature at the closest points between the two objects. The two cubes typically made initial contact edge-to-edge before rotating and assembling face-to-face. This observation also agrees with the predictions of He *et al*. [22]. An example of such a two face up cube assembly process is shown in Figs. 9(a) and 9(b). The addition of three or more cubes was found to increase the complexity of the assembly process, but the final raft nearly always formed a square lattice pattern with only a few defects typically around the edges. An example of a typical raft resulting from the assembly of 40 face up cubes is shown in Fig. 9(c).

Assemblies of cubes with an advancing contact angle of $\theta_a = 150°$, which prefer to float vertex up, were studied next. The assembly of the vertex up cubes was much more complex and varied than the face up cubes. For the face up cubes, a tight packing was achieved on the interface through a rotation around the vertical axis so that cubes could assemble face-to-face as seen in Fig. 9(a). However, for the cubes floating with their vertex up the presence of the cube beneath the surface of the water represents a physical hindrance to dense packing at the interface. As a result, the cubes which initially float with their vertex up were observed to rotate into different orientation, edge up, face up, or a tilted vertex up orientation, as they approached each other on the interface, came into contact, and assembled into a raft. Starting with two cubes floating vertex up in water, a number of prominent configurations were observed. These included cubes assembled face-to-face, vertex-to-vertex, edge-to-edge, and vertex-to-face. In Fig. 10 a histogram is presented showing the relative frequency of each of these assemblies from well over 50 individual experiments. As seen in Fig. 10, edge-to-edge assembly was the most common accounting for more than 40% of the assemblies. Face-to-face was the next most common assembly. In each of these cases, the two cubes rotate away from a vertex up orientation into an edge up orientation. In both the vertex-to-face and the less common vertex-to-vertex orientation both cubes in the final assembly maintain their vertex up alignment, although with a different tilt. The addition of three or more cubes increased the complexity of the assembly process as seen in Fig. 11. Unlike the face up cubes, the orientation and alignment of the vertex up cubes in the final particle raft was found to be quite complex and varied as the raft was build up from the many different possible orientations shown in Fig. 10. The final statistics of assembly orientation were similar in three or more cube assemblies as they were in two cube assemblies with the edge-to-edge assembly favored more than 40% of the time. Examples of some typical vertex up cube assemblies are shown in Fig. 11 both for three cubes [Figs. 11(a)–11(c)] and eight cube [Figs. 11(d) and 11(e)] assemblies. For both the face up and vertex up assemblies, the final rafts were quite

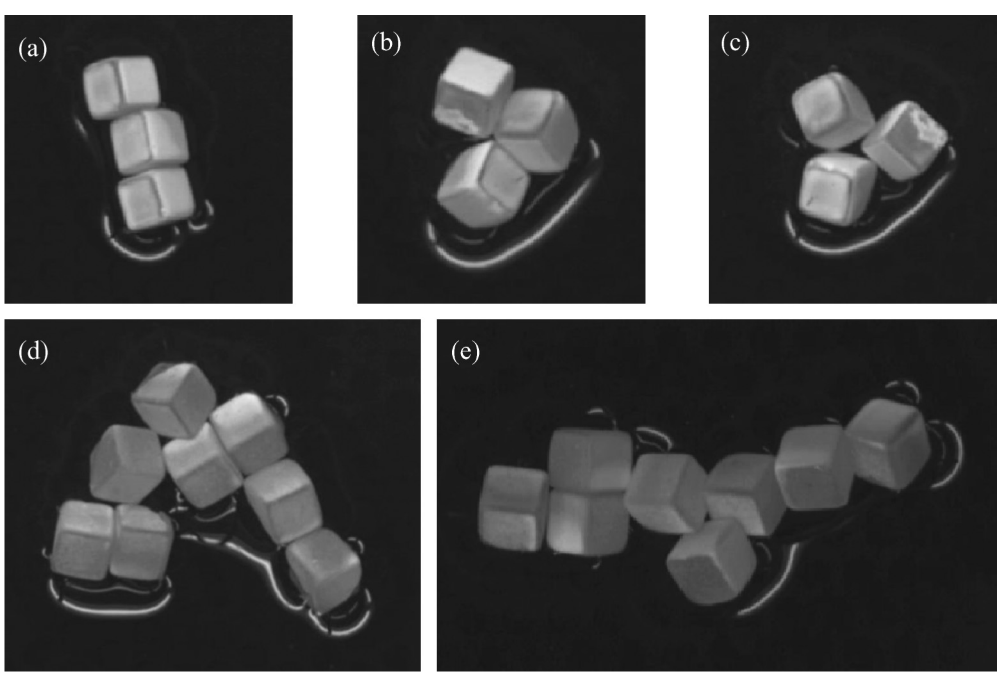

FIG. 11. Observations of three cube and eight cube assemblies for the 6.35 mm, $\theta = 150°$ cubes initially floating vertex up.

stable. Moderate disturbances produced through vibrations or interfacial waves had little impact on the arrangement and orientation of the cubes in the raft.

III. CONCLUSIONS

The effect of contact angle, density, and size on the orientation and stability of floating cubes was investigated with both experimental measurements and the development of an analytical theory. All cubes studied in these experiments were acrylic with a density of 1.16 g/cm^3, more dense than water, and were able to float because of the capillary stresses introduced by deformation of the interface at the free surface of the water. The advancing contact angle of the bare acrylic cubes was measured to be 85° which was increased to an advancing contact angle of 150° by painting the cubes with a commercially available superhydrophobic paint.

Depending on their size, density, and contact angle, the cubes were observed to float in one of three primary orientations: edge up, vertex up, and face up. A series of theoretical calculations were performed for the cubes floating in each of the three primary orientations to determine the net force on the cube. Cubes would then be expected to float in the orientation that maximizes the vertical component of the capillary force while simultaneously providing a stable center of gravity. A cube stability diagram of cube orientation as a function of cube contact angle and size was prepared from the predictions of theory. The theoretical predictions were found to be in good agreement with experimental observations on floating cubes. An experimental apparatus was constructed to measure the sum of the gravitational force, buoyancy force, and capillary forces using a force transducer as a function of cube position as it was lowered through the air-water interface at the free surface. Measurements showed that the maximum capillary forces were always experienced for the face up orientation. However, when floatation was possible in the vertex up orientation, it was found to be the most stable cube orientation because it had the lowest center of gravity. Experiments with crosses and circular cylinders showed that corners on the edge around the top face of the shape facilitated the ability of the contact line to turn the corner onto the horizontal surface of the shape, at which point the contact line advanced rapidly across the top surface, sinking the shape. For the sizes and shapes studied, the number of vertical edges had no influence on the force exerted on the cube before the contact line reached the top edge of the shape.

The assembly of cubes floating both face and vertex up were also studied for assemblies of two, three, and many cubes. Cubes floating face up were found to assemble face-to-face and form regular square lattice pattern with no free interface between cubes. Cubes floating vertex up were found to assemble in a variety of different arrangements including edge-to-edge, vertex-to-vertex, face-to-face, and vertex-to-face with the most frequent assembly being edge-to-edge. Large numbers of vertex up cubes were found to pack with a wide distribution of orientations and alignments. In all cases, assembled rafts were found to be quite stable.

ACKNOWLEDGMENT

The authors would like to thank NSF for funding this research under Grant No. CBET-0967531.

[1] E. C. Tupper, *Introduction to Naval Architecture* (Butterworth-Heinemann, Jordan Hill, GBR, 2004).
[2] E. N. Gilbert, Am. Math. Mon. **98**, 201 (1991).
[3] P. G. de Gennes, Rev. Mod. Phys. **57**, 827 (1985).
[4] J. W. M. Bush, D. L. Hu, and M. Prakash, Adv. Insect Physiol. **34**, 117 (2007).
[5] D. L. Hu, B. Chan, and J. W. M. Bush, Nature (London) **424**, 663 (2003).
[6] J. B. Keller, Phys. Fluids **10**, 3009 (1998).
[7] F. Shi, J. Niu, J. Liu, F. Liu, Z. Wang, X.-Q. Feng, and X. Zhang, Adv. Mater. **19**, 2257 (2007).
[8] X.-Y. Ji, J.-W. Wang, and X.-Q. Feng, Phys. Rev. E **85**, 021607 (2012).
[9] D.-G. Lee and H.-Y. Kim, J. Fluid Mech. **624**, 23 (2009).
[10] F.-M. Chang, Y.-J. Sheng, and H.-K. Tsao, App. Phys. Lett. **95**, 204107 (2009).
[11] D. Vella and L. Mahadevan, Am. J. Phys. **73**, 817 (2005).
[12] C. Zeng, H. Bissig, and A. D. Dinsmore, Solid State Commun. **139**, 547 (2006).
[13] P. A. Kralchevsky and K. Nagayama, Adv. Colloid Interface Sci. **85**, 145 (2000).
[14] M. G. Nikolaides, A. R. Bausch, M. F. Hsu, A. D. Dinsmore, M. P. Brenner, C. Gay, and D. A. Weitz, Nature (London) **420**, 299 (2002).
[15] S. Reynaert, P. Moldenaers, and J. Vermant, Langmuir **22**, 4936 (2006).
[16] P. Pieranski, Phys. Rev. Lett. **45**, 569 (1980).
[17] A. Moncho-Jordá, F. Martínez-López, A. E. González, and R. Hidalgo-Álvarez, Langmuir **18**, 9183 (2002).
[18] R. Aveyard, J. H. Clint, D. Nees, and V. N. Paunov, Langmuir **16**, 1969 (2000).
[19] M. Cavallaro, L. Botto, E. P. Lewandowski, and M. W. K. J. Stebe, Proc. Natl. Acad. Sci. USA **108**, 20923 (2011).
[20] H. Lehle, E. Noruzifar, and M. Oettel, Eur. Phys. J. E **26**, 151 (2008).
[21] J. C. Loudet and B. Pouligny, Eur. Phys. J. E **34**, 76 (2011).
[22] A. He, K. Nguyen, and S. Mandre, Europhys. Lett. **102**, 38001 (2013).
[23] J. Feng and J. P. J. Rothstein, Colloid Interface Sci. **354**, 386 (2011).
[24] K. A. Brakke, Exp. Math. **1**, 141 (1992).